JOURNAL OF CATALYSIS 133, 136–145 (1992)

Disproportionation Mechanism Study of Probing by *n*-Propylbenzene

TSENG-CHANG TSAI[1] AND IKAI WANG[2]

Department of Chemical Engineering, Tsing-Hua University, Hsinchu, Taiwan, Republic of China

Received January 11, 1991; revised September 5, 1991

Disproportionation of *n*-propylbenzene is proposed as a method of exploring the intrinsic reaction mechanisms and *internal* pore systems of zeolites. It was found that the reaction mechanism depends on the internal pore structure. From the distribution of dipropylbenzene isomers, the reaction mechanisms of both monomolecular and bimolecular reactions are elucidated. Only the zeolites with 12-membered rings and open pore structures undergo the bimolecular reaction mechanisms. The selectivity of dipropylbenzene ring isomers is product shape selective with respect to the size of the zeolite pore *opening*. Zeolites with bimolecular reaction mechanism exhibit higher disproportionation selectivity and catalytic stability than those with monomolecular reaction mechanism. It was determined that Zeolite beta has very open internal pore space and a loose structure.

INTRODUCTION

There are many disproportionation processes in commercial operation, including the conversion of toluene by disproportionation into xylenes and benzene (*1*), conversion of ethylbenzene by disproportionation into *p*-diethylbenzene and benzene (*2*), and conversion of toluene and trimethylbenzene by transalkylation into xylenes (*3*). In addition, cumene disproportionation for diisopropylbenzenes (*4, 5*) and trimethylbenzene disproportionation for tetramethylbenzenes and xylenes (*6*) also have potentially valuable commercial applications.

Zeolite acidity significantly affects disproportionation activity. Disproportionation of toluene (*7*), ethylbenzene (*8*), and cumene (*9*) have been developed as sensitive probe reactions for zeolite acidity.

Previous studies on the mechanism of alkylbenzene disproportionation over the $HFBF_3$ homogeneous catalysts, made by McCaulay and Lien (*10*) and also by Roberts and Roengsumran (*11*), have found that disproportionation is a bimolecular reaction at low operating severities and a monomolecular reaction at high operating severities. In heterogeneous catalysis over zeolites, pore structure would influence reaction mechanisms when the pores are comparable to the size of the molecules involved in the reactions. Pore structure effects on reaction selectivity of dialkylbenzene disproportionation were comprehensively studied by Csicsery (*12–14*). However, the study on the effects of zeolite pore structure and acidity on the disproportionation mechanisms is still very incomplete. The only earlier work was that of Amelse who used an isotope tracer technique (*15*). He found that the disproportionation mechanism is selective to zeolite pore structures. In this study, disproportionation of *n*-propylbenzene is applied as a probe reaction for mechanistic study. Effects of reaction mechanism on activity, deactivation, and coke formation are also studied. In addition, the characteristic pore structure and stability of Zeolite beta, a rarely studied but potentially useful catalyst in transalkylation (*16*) and disproportionation (*5*), are carefully examined.

EXPERIMENTAL

The Zeolite H–beta was prepared according to the procedures described by Wadlinger *et al.* (*17*) and Pererz-Pariente

[1] On leave from the Chinese Petroleum Corporation.
[2] To whom all correspondence should be addressed.

0021-9517/92 $3.00

et al. (*18*). Zeolite H-ZSM-5 was prepared using the procedures documented by Chao *et al.* (*19*). Zeolite NH_4Y (H–Y) and H–mordenite were supplied by the Strem Chemicals Co. Zeolite H–ultrastable Y (H–USY) and high siliceous H–mordenite (H–UM) were supplied by the Tosoh Co.

Reactions were conducted in a continuous fixed-bed reactor system. Mixtures of 12–20 mesh, 2.54 g zeolite, and 4.65 g ceramics were packed into the reactor and activated in air 6 h at 723°K. The reactor was then cooled under a nitrogen stream down to the desired temperatures of disproportionation experiments.

Using a metering pump, *n*-propylbenzene (Merck) was delivered into the reactor without purification. The reaction products were collected in 15-min intervals and analyzed with a Hewlett–Packard Model 5840A gas chromatograph, equipped with a squalene capillary column.

The conversion of *n*-propylbenzene, X_p, is defined by

$$X_p = 100 - ((M), \text{wt}\%)_p \qquad (1)$$

where $(M, \text{wt}\%)_p$ is the composition of *n*-propylbenzene in the reactor effluents.

Upon completion of the disproportionation experiments, the catalysts were purged with nitrogen 3 h at the reaction temperature. The amount of coke deposition was then measured using a Dupont 951 Thermogravimeter.

RESULTS AND DISCUSSION

A. *Disproportionation Reaction Mechanisms*

Disproportionation of monoalkylbenzenes can follow either the S_{N_2} mechanism (bimolecular reaction) or the S_{N_1} mechanism (monomolecular reaction (Fig. 1). In the S_{N_2} mechanism, alkylbenzene first forms a carbenium ion, then a biphenylmethane-type intermediate, and finally dissociates into dialkylbenzenes and benzene (*12, 20*). In the S_{N_1} mechanism, alkylbenzene first cracks into an alkyl ion and a benzene molecule. The former then alkylates another alkylbenzene and forms dialkylbenzenes. Previous studies over HF-BF_3 (*10, 11*) have shown that at low reaction temperatures the S_{N_2} mechanism dominates while at high reaction temperatures the S_{N_1} mechanism dominates.

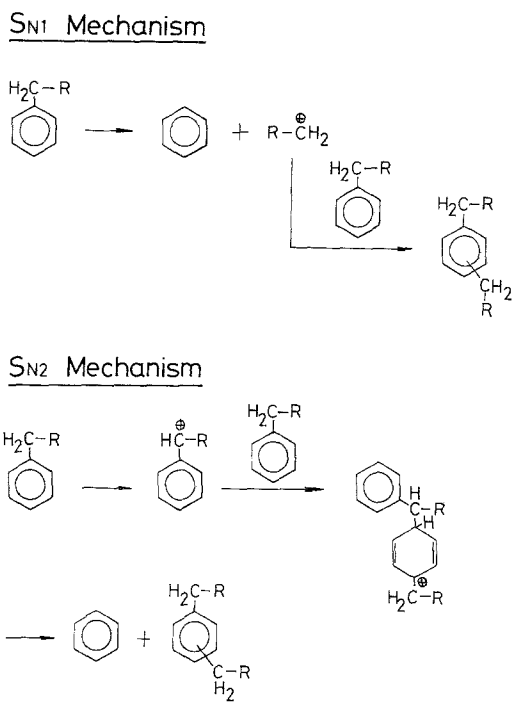

FIG. 1. Disproportionation reaction mechanisms.

In this study, we find that *n*-propylbenzene disproportionation is a useful probe reaction for distinguishing reaction mechanisms (Fig. 2). By examining the fraction of dipropylbenzene isomers, one can identify not only the reaction mechanisms but also the product shape selectivity. Disproportionation of *n*-propylbenzene gives mainly benzene and dipropylbenzene (DPB) products. DPB has three alkyl group isomers, *n*-propyl-*i*-propyl-benzene (*ni*PB), di-*n*-propylbenzene (*nn*PB), and diisopropylbenzene (*ii*PB). The fractional distribution of alkyl group isomers can be used to determine whether the reaction mechanism is S_{N_2} or S_{N_1}. In addition, each DPB has its own three-ring position isomers, *o*-, *m*-, and

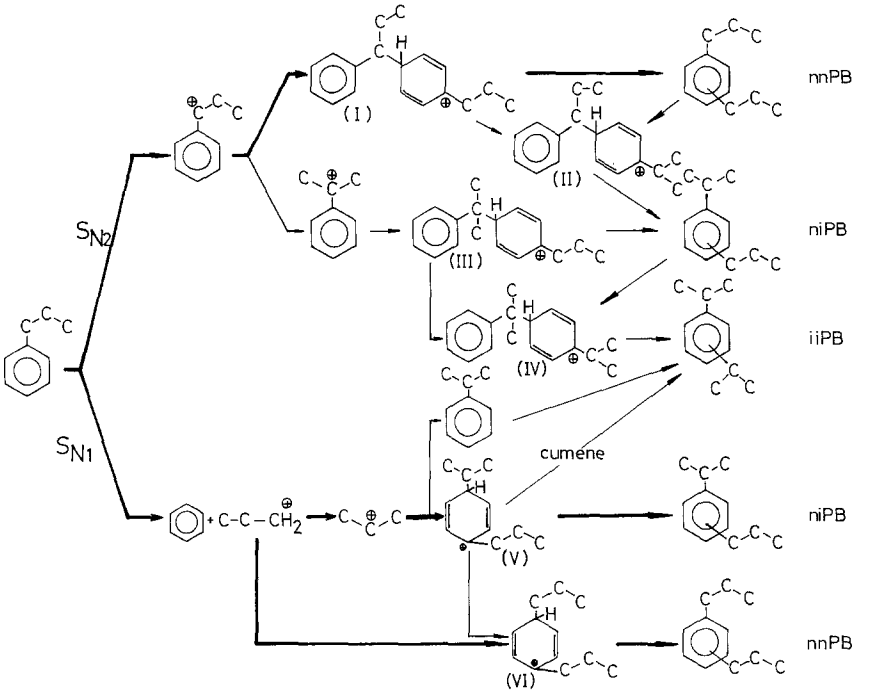

FIG. 2. Reaction mechanisms of *n*-propylbenzene disproportionation (—— major path; —— minor path).

p-isomers. The shape selectivity of *p*-dipropylbenzene (*p*-DPB) can be properly correlated to the pore sizes of zeolites.

The stability of the carbocations decreases in the order tertiary > secondary > primary ions. For the S_{N_1} mechanism, prior to propyl group transfer, the *n*-propyl group of *n*-propylbenzene is severed from the aromatic ring. Over acid zeolites, these *n*-propyl ions can isomerize to *i*-propyl ions. The equilibrium is reached very rapidly. Hence, the primary products are *ni*PB and *nn*PB. However, with the S_{N_2} mechanism, no free propyl ions are formed. The primary products produced from the biphenylmethane intermediates are mainly *nn*PB. Consequently, from the relative fractions of *nn*PB and *ni*PB in the product, conclusion regarding the operative mechanism (S_{N_1} or S_{N_2}) can be made.

The disproportionation of *n*-propylbenzene over various zeolites was conducted at reaction temperatures of 473 ± 1 K with low conversion levels of 5 ± 0.5%, so that intrinsic disproportionation mechanisms on different zeolites could be explored (Table 1). In this experiment, zeolite samples with crystal sizes larger than 1 μm were chosen to minimize the interference from disproportionation on the external surface. According to DPB isomer distribution, the zeolites studied can be classified into three categories (Table 1 and Fig. 3a). Zeolite beta and USY, belong to the first category in which disproportionation products are predominantly *nn*PB. ZSM-5, belongs to the second category in which equal moles of *nn*PB and *ni*PB are produced. Mordenite belongs to the third category whose *nn*PB fraction lies between that of the other two categories.

The zeolites with larger pores preferentially produce *nn*PB, which has a molecular diameter smaller than that of *ni*PB. The preference for *nn*PB formation decreases in the order of USY > beta > mordenite > ZSM-

TABLE 1

Comparison of Zeolites in *n*-Propylbenzene Disproportionation at 473 ± 3°K and Low Conversion Levels[a]

	H-Beta	H-USY	HUM	HZSM-5
SiO_2/Al_2O_3 (mol/mol)	36.0	14.0	19.0	45.0
Crystal size (μm)	1.2	1.5	1.0	4.0
Crystal shape	Polyhedra	Sphere	Long rice	Sphere
Rx. temperature (K)	472	473	472	473
WHSV (g/g cat h)	6.7	6.2	2.0	2.7
Conversion (wt%)	5.13	4.96	5.47	4.96
Selectivity (mol/mol)				
S_D	0.94	0.94	0.75	0.73
Benzene/DPB	1.03	1.02	1.23	1.23
DPB isomer distribution				
*nn*PB/DPB	0.97	1.00	0.74	0.50
*ni*PB/DPB	0.03	0	0.26	0.50
*ii*PB/DPB	0	0	0	0
*p/m-nn*PB	0.65	0.89	0.68	1.00
*p/m-ni*PB	0.59	—	0.49	∞
Product yields (wt%)				
C_6^- Light Gas	0.10	0.05	0.20	0.17
Benzene	1.61	1.55	1.63	1.45
Toluene + xylene	0.04	0.11	0.36	0
Cumene	0.02	0	0.14	0.26
n-Propylbenzene	94.87	95.04	93.53	95.04
C_{10} + C_{11} aromatics	0.11	0.11	0.38	0.64
*m-ni*PB	0.06	0	0.49	0
*p-ni*PB	0.03	0	0.24	1.21
*m-nn*PB	1.92	1.66	1.21	0.61
*p-nn*PB	1.24	1.50	0.83	0.61

[a] Time-on-stream: 60 min.

5. These results can be explained by the hypothesis that, due to inadequate internal pore space required for the formation of biphenylmethane intermediates in the S_{N_2} mechanism (Fig. 2), ZSM-5, a 10-membered ring zeolite, catalyzes the S_{N_1} mechanism. In the other extreme, Zeolite Y with a large supercage of 13 Å in diameter has the highest *nn*PB distribution. Therefore, we conclude that disproportionation mechanisms are shape selective to the *internal pore structures* of zeolites. The same conclusion was drawn by Amelse from disproportionation experiments over Zeolite Y and a 10-membered ring zeolite, AMS-1B, using an isotope tracer technique (*15*). However, the combined mechanism on mordenite has not been previously discussed.

The framework structure of zeolite beta was disclosed by Higgins *et al.* (*21*). The internal pore structure of zeolite beta is still not fully understood, owing to its highly faulted structures. Based on the *nn*PB fraction, we believe that the order of internal pore space decreases as USY > beta > mordenite > ZSM-5.

Moreover, *p*-DPB selectivity, as expressed in the ratios of *p/m-nn*PB, and *p/m-ni*PB, strongly depends on the pore opening of zeolites (Table 1). The *p/m*-DPB ratios of zeolite beta, USY, and mordenite are all significantly less than ZSM-5, which has the smallest pore opening among the zeolites studied (Table 2). Therefore, the distribution of DPB ring isomers is controlled by product shape selectivity. The high *p/m-nn*PB ratio of USY could be attributed to

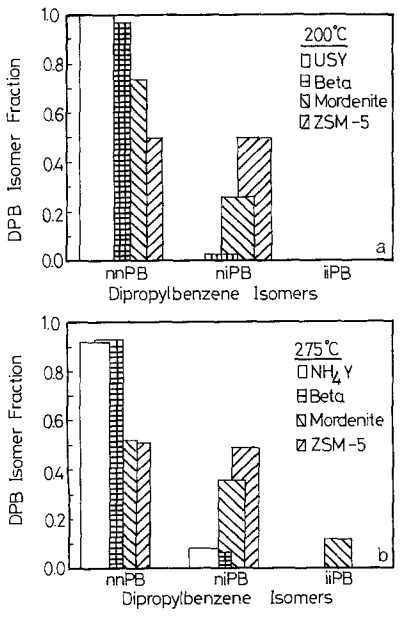

FIG. 3. Comparison of distribution of dipropylbenzene isomers over different zeolites at reaction temperatures of (a) 473°K and (b) 548°K.

the high diffusivity of *p-nn*PB that minimizes the secondary isomerization.

When disproportionation selectivity is 100 mol%, 2 mol of *n*-propylbenzene should produce 1 mol of benzene and DPB. If cracking reaction takes place as secondary or parallel reactions to the disproportionation reaction, excess benzene will be obtained and the benzene-to-DPB ratio (B/DPB) will be above unity. Accordingly, selectivity of disproportionation, S_D, is defined as

$$S_D = \frac{2(\text{DPB, wt\%}|_p/162)}{X_p/120}, \qquad (2)$$

where $(\text{DPB, wt\%})_p$ is DPB yield.

The zeolites with S_{N_2} mechanism catalyze greater S_D than the zeolites with S_{N_1} mechanism (Table 1). This is consistent with the difference in the nature of their reaction paths. In the S_{N_2} mechanism, which Zeolites beta and Y catalyze, approximately equal moles of benzene and DPB are formed. But in the S_{N_1} mechanism (which ZSM-5 catalyzes), propyl ions are cracked prior to propyl group transfer. The B/DPB ratio of S_{N_1} mechanism will, hence, be larger than unity. For ZSM-5 and mordenite, two zeolites with high S_{N_1} degree, the cumene yield is higher than that for the zeolites following the S_{N_2} mechanism (Table 1). Similarly, the $C_9 + C_{10}$ aromatic yields over S_{N_1} zeolites are much greater than that over S_{N_2} zeolites. The preference for the formation of benzene, cumene, and $C_9 + C_{10}$ aromatics over S_{N_1} zeolites results in their low S_D.

The dependence of S_D and *nn*PB fraction on reaction temperature varies with zeolite type (Fig. 4). At all temperatures studied, the *nn*PB fraction is the greatest for USY and the lowest for ZSM-5 (Fig. 4a). For ZSM-5, the S_D and *nn*PB are independent of reaction temperatures. In the S_{N_1} mechanism, cracking occurs in the initial steps; therefore, reaction temperatures would not be expected to influence the disproportionation selectivity over ZSM-5. The results demonstrated that for S_{N_1} mechanism, at very low conversion levels like 5 wt%, the

TABLE 2

Zeolite Structures

Zeolite	Pore structure	Pore opening (Å)	F_D[a]
ZSM-5	Interconnecting, three dimensional	5.4*5.6, 5.1*5.5	17.9
Mordenite	Interconnecting, two dimensional	6.5*7.0, 2.6*5.7	17.2
Beta	Interconnecting, three dimensional	7.5*5.7, 6.5*5.6	—
Y	Three dimensional	7.4	12.7

[a] Framework density in $T/1000$ Å^3.

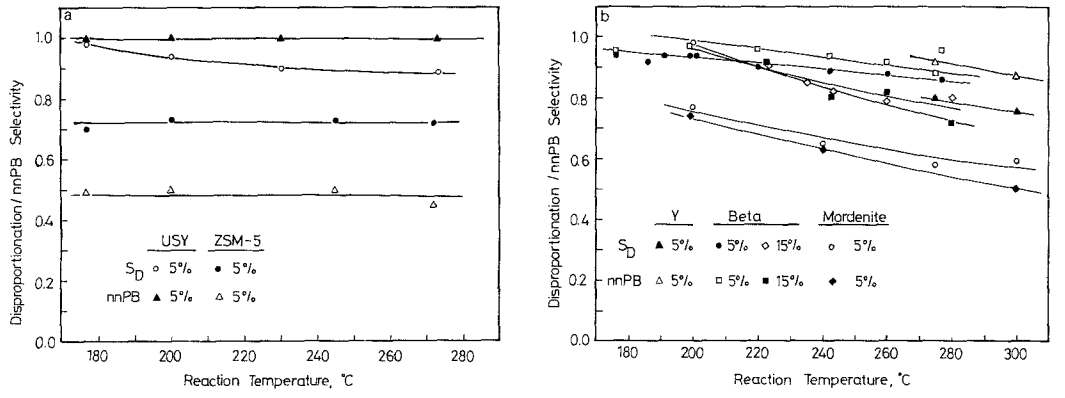

FIG. 4. Plot of disproportionation selectivity and di-*n*-propylbenzene fraction over different zeolites against reaction temperatures.

*ni*PB-to-*nn*PB distribution remains essentially constant over wide operating conditions. This is possible because in the S_{N_1} mechanism the concentration of *n*-propyl ions and *i*-propyl ions reach thermodynamic equilibrium. For USY with S_{N_2} mechanism, the *nn*PB fraction and the degree of S_{N_2} mechanism remain high and did not vary with operating temperatures.

However, for Zeolites beta and Y, both S_D and *nn*PB fraction decline slightly with increasing reaction temperatures (Fig. 4b). Furthermore, high reaction temperatures would favor cracking reactions and shift the reaction mechanism from S_{N_2} to S_{N_1}. As expected, decline of *nn*PB formations and S_D was observed (Fig. 4b).

To quantify the degree of S_{N_1} and S_{N_2} mechanism, the following analytical model is proposed. In S_{N_1} mechanism, the *nn*PB fraction equals 0.50. In S_{N_2} mechanism, *nn*PB fraction equals 1.0. Accordingly, the degree of those two mechanisms can be segregated by simple linear equations,

$$S_{nnPB} = S_1(0.50) + S_2(1) \quad (3)$$

$$S_1 + S_2 = 1, \quad (4)$$

where S_{nnPB} is the experimental *nn*PB fraction, S_1 and S_2 are the *degree* of S_{N_1} and S_{N_2} mechanism, respectively.

For example, over mordenite, the following results are abstracted from Tables 1 and 4:

Reaction temperatures (K)	472	548
Conversion (wt%)	5.47	5.37
*nn*PB distribution	0.74	0.52

By Eqs. (3) and (4), we obtain

At 472 K,

$$0.74 = (1 - S_2)(0.50) + S_2$$

$$S_2 = (0.74 - 0.50)/0.50 = 0.48 \quad (5)$$

$$S_1 = 1 - 0.48 = 0.52$$

At 548 K,

$$0.52 = (1 - S_2)(0.50) + S_2$$

$$S_2 = (0.52 - 0.50)/0.50 = 0.04 \quad (6)$$

$$S_1 = 0.96.$$

Therefore, we obtain

Reaction temperatures (K)	472	548
S_1	0.52	0.96
S_2	0.48	0.04

A similar calculation was performed for each studied zeolite and the results were tabulated in Table 3. Note that regardless of operating temperatures, ZSM-5 has S_1 of 1.0 and USY has S_2 of 1.0, indicating that ZSM-5 proceeds by the S_{N_1} mechanism and USY undergoes the S_{N_2} mechanism. At reaction temperatures of 473 K, Zeolite Y and beta, with 12-membered ring and open pore struc-

TABLE 3

Intrinsic Disproportionation Selectivity of S_{N_1} and S_{N_2} Mechanism

Zeolites	Beta		USY		Mordenite		ZSM-5
SiO_2/Al_2O_3	15	36	2.1	14	19	22.9	45
	Mechanism selectivity						
At 473°K							
S_{N_1} Mechanism	0.08	0.06	—	0	0.52	0.36	1.0
S_{N_2} Mechanism	0.92	0.94	—	1.0	0.48	0.64	0
At 548°K							
S_{N_1} Mechanism	0.16	0.14	0.16	0	0.96	0.78	1.0
S_{N_2} Mechanism	0.84	0.86	0.84	1.0	0.04	0.22	0

tures, obtain S_2 of nearly 1.0 and, therefore, their reaction mechanisms are S_{N_2} dominant. However, mordenite, a 12-membered ring zeolite with restricted pore structure (*22*), possesses nearly equal S_1 and S_2, indicating that mordenite catalyzes a combined S_{N_1} and S_{N_2} mechanism. As shown in Fig. 4b and Table 3, mordenite beyond 549 K undergoes the S_{N_1} dominant mechanism.

At higher temperatures, the contribution of the S_{N_2} mechanism decreases and that of the S_{N_1} mechanism increases (Table 3). The same conclusions can be also drawn for Zeolite beta (Fig. 5).

The dependence of S_D and *nn*PB fraction with conversion levels was studied over Zeolite beta at a constant reaction temperature of 473 K (Fig. 6). With increasing conversion levels, S_D remains essentially unchanged and *nn*PB fraction decreases only slightly. At high conversion levels, the secondary isomerization from complex (I), *nn*PB carbenium ions, or *nn*PB could take place to form *ni*PB and *ii*PB and reduce the *nn*PB fraction, while the reaction mechanism remains the same.

The intrinsic mechanisms were further explored at reaction temperatures of 548 K and low conversion levels (Table 4). The conclusions drawn from Table 1 that the preference of the formation of *nn*PB can be

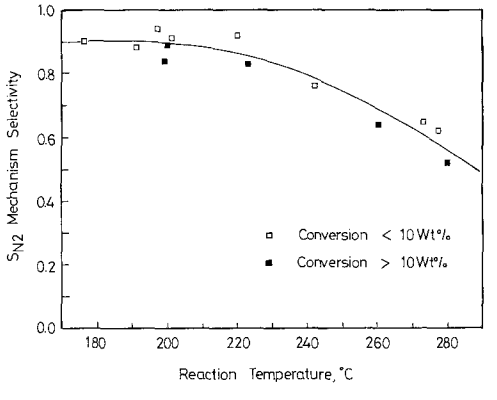

FIG. 5. Plot of S_{N_2} mechanism selectivity over zeolite beta against reaction temperatures at different conversion levels at wide operating range (temperature: 449–553°K; WHSV: 1.4–42.8 g h^{-1} g cat^{-1}).

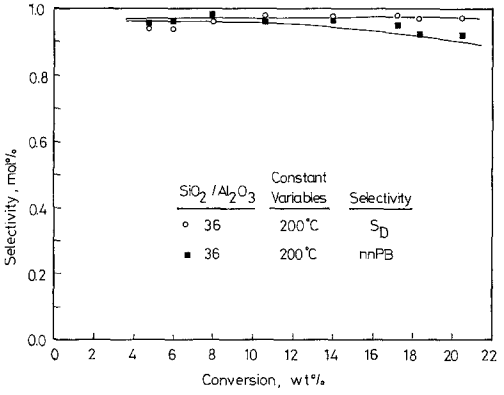

FIG. 6. Plot of disproportionation selectivity and nnPB fraction over zeolite beta against conversion levels at a constant temperature of 473°K.

TABLE 4

Comparison of Zeolites in *n*-Propylbenzene Disproportionation at 548 ± 3°K and Low conversion Levels[a]

	H-Beta	HY		HM		HZSM-5	
SiO_2/Al_2O_3 (mol/mol)	36.0	2.1	14.0	19.0	21.0	45.0	35.8
Crystal size (μm)	1.2	1.5	1.5	1.0	1.0	4.0	0.1
Crystal shape	Polyhedra	Polyhedra	Sphere	Long Rice	Corn	Sphere	Sphere
Rx. temperature (K)	550	548	546	548	548	548	545
WHSV (g/g cat h)	42.8	2.1	53.0	3.4	50	8.0	35.7
Conversion (wt%):	4.70	4.62	4.4	5.37	4.75	5.0	4.99
Selectivity (mol/mol)							
S_D	0.86	0.80	0.89	0.58	0.61	0.72	0.72
Benzene/DPB	1.04	1.06	1.02	2.23	1.37	1.28	1.20
DPB isomer distribution							
nnPB/DPB	0.93	0.92	1.0	0.52	0.61	0.51	0.45
niPB/DPB	0.07	0.08	0	0.36	0.39	0.49	0.55
iiPB/DPB	0	0	0	0.12	0	0	0
p/m-nnPB	0.48	0.46	0.74	0.49	1.08	3.13	0.88
p/m-niPB	0.68	0.75	—	0.49	0.50	∞	3.32
p/m-iiPB	—	—	—	0.47	—	—	—
Stability							
$y * 1000$	2.5	1.9	0.2	24.4	22.0	3.5	3.0
Product yields (wt%)							
C_6^- Light Gas	0.27	0.31	0.17	0.30	0.15	0.18	0.20
Benzene	1.35	1.28	1.29	2.26	1.29	1.50	1.40
Toluene	0	0.20	0	0.20	0.26	0.01	0
Cumene	0.09	0.04	0	0.25	0.25	0.11	0.33
n-Propylbenzene	95.3	94.38	95.61	94.63	95.25	95.00	95.01
C_{10} + C_{11} aromatics	0.26	0.28	0.31	0.24	0.85	0.80	0.62
*m-ii*PB	0	0	—	0.17	—	0	0
*p-ii*PB	0	0	—	0.08	—	0	0
*m-ni*PB	0.34	0.12	—	0.51	0.52	0	0.31
*p-ni*PB	0.23	0.09	—	0.25	0.25	1.19	1.03
*m-nn*PB	1.45	1.57	1.50	0.74	0.57	0.30	0.58
*p-nn*PB	0.70	0.72	1.12	0.36	0.62	0.94	0.51

[a] Time-on-stream: 60 min.

found for S_{N_2} zeolites and that the *p*/*m*-DPB ratios depend on pore opening, still hold true. In addition, over Zeolite Y and mordenite, the S_D, *nn*PB, and *p*-DPB selectivity increase with SiO_2/Al_2O_3. However, the difference of disproportionation selectivity between S_{N_2} and S_{N_1} zeolites at high temperatures becomes less significant (Table 4 and Fig. 4b).

The effects of crystal size of ZSM-5 are presented in Table 4. The increase in external surfaces as a result of reducing crystal sizes would favor secondary isomerization and external surface disproportionation. The activity of ZSM-5 with 4 μm is lower than that with 0.1 μm, indicating that over ZSM-5, *n*-propylbenzene disproportionation is a diffusion-controlled reaction. Because it has a smaller molecular size than *ni*PB, *nn*PB could diffuse out from internal pores faster and undergo secondary isomerization on the external surface. Therefore, with reducing crystal sizes, *ni*PB fraction increases and exceeds the thermodynamic equilibrium *ni*PB fraction, 0.50. The increase of the fraction of the external surface with decreasing crystal sizes also results in the decrease of *p*-DPB selectivity, as expressed in *p*/*m-nn*PB and *p*/*m-ni*PB ratios.

The effects of operating conditions on re-

TABLE 5

Summary of Effects of Operating Conditions on Selectivity of Disproportionation and Reaction Mechanisms

	Temperatures	WHSV	Conversion	S_D	*nn*PB Fraction
	⇒	⇓	⇑	⇒	=
	⇑	⇒	⇑	⇓	⇓
5% Conversion	⇑	⇑	⇒	⇓	=
15% Conversion	⇑	⇑	⇒	⇓	⇓

action mechanism are summarized in Table 5. First, with increasing conversion levels and decreasing space velocity, at a constant reaction temperature, S_D remains constant and *nn*PB fraction decreases, due to secondary isomerization. Second, raising conversion levels by raising reaction temperatures, at a constant space velocity, both S_D and *nn*PB distribution decrease, which is due to shift of reaction mechanisms from S_{N_2} to S_{N_1}. Third, raising reaction temperatures and space velocity, at constant low conversion levels of 5%, resulted in a decrease of S_D and a slight decline of *nn*PB fraction. This is due to the shift from S_{N_2} to S_{N_1}. Fourth, at high conversion levels of approximately 15%, the decreases in *nn*PB fraction become more pronounced, due to secondary isomerization. In conclusion, S_D depends primarily on reaction temperature while the *nn*PB fraction depends on both the reaction temperature and conversion levels.

Weitkamp *et al.* (*22*) designated a spaciousness index (SI), which was measured from a hydrocracking reaction of C_{10}–naphthene, to elucidate the *effective* pore openings of zeolites. By SI scale, the 12-membered ring zeolites with restricted pore systems, such as mordenite and ZSM-12, can be distinguished from those with wide open pores. Here, the *n*-propylbenzene disproportionation is demonstrated as in another diagnosis test providing the similar function. By examining disproportionation mechanisms, it is found that the *internal* pore size of mordenite is marginal for catalyzing disproportionation reactions by a pure S_{N_2} mechanism.

Both the SI test and this study are based on the selectivity of reaction intermediates. The SI test examines the cracking selectivity of exocyclic ions while *n*-propylbenzene disproportionation inspects the transfer selectivity of propyl groups. As shown from both studies, Zeolite beta has very open *internal* pore systems.

B. Effect of Reaction Mechanisms on Activity and Stability

By infrared red spectroscopy, Hedge *et al.* (*23*) reported that the acidity decreases in order as ZSM-5 > beta > Y. However, the activity of *n*-propylbenzene disproportionation activity of Zeolite beta is slightly greater than ZSM-5 and the zeolite activity decreases in order as beta > ZSM-5 > mordenite > Y (Table 4). There are two possible reasons for the inconsistency between acidity and activity for Zeolite beta and ZSM-5. First, the S_{N_1} and S_{N_2} require the cracking of propyl groups in the monoalkylbenzenes and biphenylmethane intermediates respectively. Second, over ZSM-5 *n*-propylbenzene disproportionation is diffusion controlled and influenced by crystal sizes. Therefore, Zeolite beta with its 12-membered ring pores is in an advantageous position. In addition, activity of zeolite mordenite and Y increases after dealumination treatment. Similar results have been reported by Csicsery (*13*) and Karge *et al.* (*24*). Karge *et al.* (*24*) attributed the activity enhancement to the increases of adsorption rates of the dealuminated zeolites.

Catalytic decay can be correlated to the

time-on-stream (TOS) by using the exponential function,

$$X_t = X_0 e^{-yt}, \qquad (7)$$

where X_t is the conversion at TOS of t; y is a decay exponent. The higher the y is, the lower the stability is.

Zeolite stability in *n*-propylbenzene disproportionation is shown in Table 4. Although ZSM-5 is a well-known stable catalyst, poor stability was observed in this reaction. The stability of Zeolite beta and Y are higher than that of mordenite and ZSM-5. In the previous studies, Guisnet and Magnoux (*25*) have correlated cracking stability of zeolites with their pore structures. Here we find that catalytic deactivation is also closely affected by reaction mechanisms.

CONCLUSION

Disproportionation of *n*-propylbenzene is demonstrated to be a useful diagnostic tool to probe the *internal* pore systems of zeolites. The disproportionation reactions proceed through the monomolecular S_{N_1} reaction mechanism in ZSM-5. Over Zeolites beta and Y, the bimolecular S_{N_2} mechanism prevails. Both mechanisms prevail in the unidimensional pore system of mordenite. Dealumination can enhance S_{N_2} mechanism selectivity. Both the disproportionation selectivity and catalytic stability are higher over zeolites wherein the S_{N_2} mechanism prevails than over those with S_{N_1} mechanism. The relative concentration of the various dipropylbenzene ring isomers is controlled by the size of zeolitic pore opening.

ACKNOWLEDGMENTS

We are indebted to C. Y. Chang for identification of disproportionation reaction products with GC mass spectrometer, to A. F. Hsiao for elemental analyses of zeolite samples with ICP spectrometer, and to the Tosoh Co. for the supply of USY and mordenite samples.

This research was supported by the National Science Council, Republic of China.

REFERENCES

1. Grandio, P., Schneider, F. H., Schwartz, A. B., and Wise, J. J., *Hydrocarbon. Process.* **8,** 85 (1972).
2. Wang, I., Ay, C. L., Lee, B. J., and Chen, M. H., *in* "Proceedings, 9th International Congress on Catalysis, Calgary, 1988" (M. J. Phillips and M. Ternan, Eds.), p. 324. Chem. Institute of Canada, Ottawa, 1988.
3. Hatch, L. F., and Mater, S., *Hydrocarbon. Process.* **58**(1), 189 (1979).
4. Kaeding, W. W., *J. Catal.* **120,** 409 (1989).
5. Tsai, T. C., and Wang, I., *Appl. Catal.*, in press.
6. Seitetsu, S., J. P. Pat. 4,9007,231 (1974).
7. Benesi, H. A., *J. Catal.* **8,** 368 (1967).
8. Karge, H. G., Sarbak, Z., and Hatada, K., *J. Catal.* **82,** 236 (1983).
9. Absil, R. P. L., Butt, J. B., and Dranoff, J. S., *J. Catal.* **85,** 415 (1984).
10. McCaulay, D. A., and Lien, A. P., *J. Am. Chem. Soc.* **75,** 2411 (1953).
11. Roberts, R. M., and Roengsumran, S., *J. Org. Chem.* **46,** 3689 (1981).
12. Csicsery, S. M., *J. Catal.* **23,** 124 (1971).
13. Csicsery, S. M., *Zeolites* **4,** 202 (1984).
14. Csicsery, S. M., *J. Catal.* **108,** 433 (1987).
15. Amelse, J. A., *in* "Studies in Surface Science and Catalysis," Vol. 38, p. 165, 1988.
16. Wang, I., Tsai, T. C., and Huang, S. T., *Ind. Eng. Chem. Res.* **29,** 2005 (1990).
17. Waldinger, R. L., Kerr, G. T., and Rosinski, E. J., U.S. Pat., 3,308,069 (1967).
18. Pererz-Pariente, J., Marten, J. A., and Jacobs, P. A., *Appl. Catal.* **31,** 35 (1987).
19. Chao, K. J., Tsai, T. C., Chen, M. S., and Wang, I., *J. Chem. Soc. Faraday Trans. 1* **77,** 547 (1981).
20. Roberts, R. M., Lin, Y. L., and Anderson, G. P., Jr., *Tetrahedron* **25,** 4173 (1969).
21. Higgen, J. B., Lappierre, R. B., Schlenker, J. L., Wood, A. C., Kerr, G. T., and Rohrbaugh, W. J., *Zeolites* **8,** 446 (1988).
22. Weitkamp, J., Ernst, S., and Kumar, R., *Appl. Catal.* **27,** 207 (1986).
23. Hedge, S. M., Kumar, R., Bhat, R. N., and Ratnasamy, P., *Zeolites* **9,** 231 (1989).
24. Karge, H. G., Ladebeck, J., Sarbak, Z., and Hatada, K., *Zeolites* **2,** 94 (1982).
25. Guisnet, M., and Magnoux, P., *Appl. Catal.* **54,** 1 (1989).